Table 2 NFAT consensus binding sequence identified in BPAG1 promoter

NFAT		Consensus sequence								
		T							A	
			G	G	A	A	A	A	T	N
		A						N	C	
BP-P	−291	T	G	G	A	A	A	G	G*	A
BP-M	−599	T	G	G	A	A	A	A	A	G
BP-D	−886	A	G	G	A	A	A	A	T	A

Sequences homologous to NFAT consensus motif were identified in the region of −291 to −299 (BP-P), −599 to −607 (BP-M), and −886 to −894 (BP-D) in the BPAG1 promoter region. Asterisk denotes mismatch nucleotide.

2.6. Statistical analysis

Data are expressed as means ± standard deviation (S.D.) of three independent experiments. Statistical analysis was performed with Student's *t*-test. $^{*}p < 0.01$, $^{**}p < 0.05$.

3. Results

3.1. RT-PCR analysis of NFAT expression in NHEK, NHDF, and NHEM

We first investigated the expression of NFATs by RT-PCR using total RNA extracted from cultured NHEK, NHDF, and NHEM. We detected mRNA for all NFATs in the three cell lines examined (Fig. 1). Each PCR product obtained in this study was identified by sequence analysis.

3.2. Effect of CsA on NFATs and BPAG1 expression in NHEK

To examine the effect of CsA on the expression of various NFATs and BPAG1, RT-PCR was performed using total RNA extracted from NHEK after 24 h incubation with 10^{-6} M CsA. The numbers of PCR cycles for each transcript were adjusted to yield semi-quantitative assessment of the mRNA level in the linear range of PCR. CsA treatment markedly decreased the expression of NFAT1 and NFAT2 mRNA, whereas transcripts of NFAT3, NFAT4, and NFAT5 were not (Fig. 2a and b). CsA reproducibly caused a small but significant reduction in the expression of BPAG1. The expression levels of involucrin mRNA were significantly decreased by CsA. Western analysis demonstrated that BPAG1 protein expression was significantly decreased by 10^{-6} M CsA (Fig. 2c).

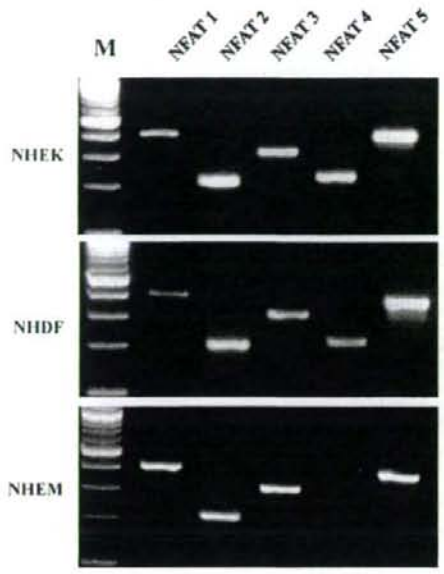

Fig. 1 Expression of NFAT family members in NHEK, NHDF, and NHEM. RT-PCR using 0.5 μg of total RNA extracted from cultured normal human epidermal keratinocytes (NHEK), normal human fibroblasts (NHDF), and normal human epidermal melanocyte (NHEM) as template, was performed with primers designed for unique sequences in different NFATs (see Table 1). M, molecular marker.

3.3. Effect of CsA on BPAG1 promoter activity in NHEK

The plasmid pBP1.9luc, which contains BPAG1 promoter region (−1908 to −1) in front of the luciferase reporter gene, was transiently transfected into NHEK cultured in KGM medium containing various concentrations of CsA, and luciferase assays were performed after 6 h of incubation. CsA in 10^{-6} or 10^{-7} M concentration clearly decreased BPAG1 gene promoter activity, which however returned to the control level at 24-h point (Fig. 3). The promoter activity was not altered at 6 h of incubation with 10^{-8} M CsA, but after 12 h CsA significantly down-regulated the promoter activity. Interestingly, the promoter activity was somewhat upregulated at 24-h point of incubation as compared to the controls (Fig. 3).

3.4. Identification and characterization of the NFAT consensus sequences in the BPAG1 gene promoter

To determine whether NFAT consensus sequences are capable of binding NHEK nuclear proteins, electro-

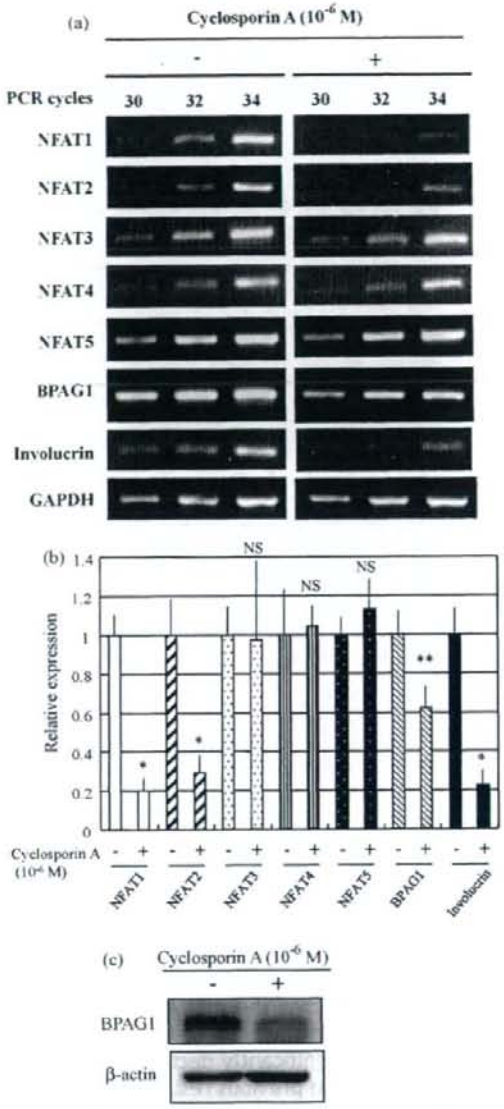

Fig. 2 Effect of CsA on NFAT and BPAG1 expression in NHEK. (a) Total RNA was extracted from NHEK incubated in the presence of CsA (10^{-6} M), and expression of NFATs, BPAG1, and involucrin was determined by semi-quantitative RT-PCR after 24-h incubation. (b) The mRNA levels of NFATs, BPAG1, and involucrin (32 cycle) quantified by densitometry and corrected for the levels of GAPDH in the same samples are shown relative to the levels in untreated cells. $^{*}p < 0.01$, $^{**}p < 0.05$. NS, not significant. (c) CsA treatment for 48 h reduced the BPAG1 protein expression.

phoretic gel mobility shift assays were performed using a 28-bp oligonucleotide DNA which includes NFAT consensus sequence of the IL-2 gene promoter region (ARRE-2), previously shown to exhibit NFAT

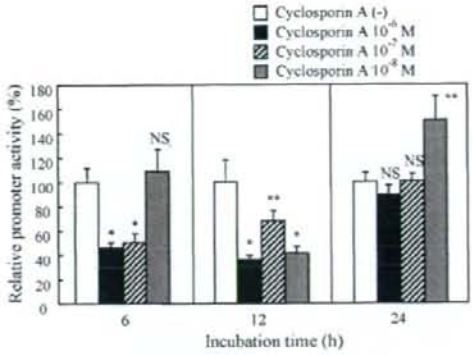

Fig. 3 Effect of CsA on BPAG1 promoter activity. Plasmid pBP1.9luc, which contains BPAG1 promoter region (−1908 to −1) in front of the luciferase reporter gene, was transiently co-transfected with CMV-lacZ plasmid into NHEK cultured in KGM medium containing various concentrations of CsA. Six to 24 h after transfection, luciferase assays were performed, and the values were normalized using β-galactosidase activity in the same samples. Note that CsA reversibly downregulated transcription of the BPAG1 promoter. Data are expressed as mean ± S.D. of three independent experiments in duplicate. Statistical analysis was performed with Student's *t*-test. $^{*}p < 0.05$, $^{**}p < 0.01$. NS, not significant.

binding activity [12–15]. Although several shifted bands were detected, one band with specific NFAT binding activity was identified (Fig. 4). This band was displaced by the addition of a specific, unlabeled competitor, but was not influenced by non-specific competitors (Fig. 4A). When NFAT binding activity was examined with probes containing BP-P, BP-M, and BP-D sequences, as identified in the BPAG1 promoter region, specific binding activities similar to those described for ARRE-2 were detected with BP-M and BP-D probes (Fig. 4B). Thus, these two regions may act as NFAT binding elements for BPAG1 gene promoter.

4. Discussion

In the present study, we demonstrated mRNA expression of all NFAT family members NFAT1, 2, 3, 4, and 5 in cultured human epidermal keratinocytes, fibroblasts, and melanocytes (Fig. 2a). In addition, our results showed that CsA downregulates the expression of NFAT1 and NFAT2. These results suggest that transcriptional regulation of NFATs might be directly involved in the calcineurin/NFAT system in human keratinocytes. Previous works have revealed that CsA inhibits nuclear translocation of NFAT1 in human keratinocytes in vivo and in vitro [4] and in mouse follicular keratinocytes in vivo [6].

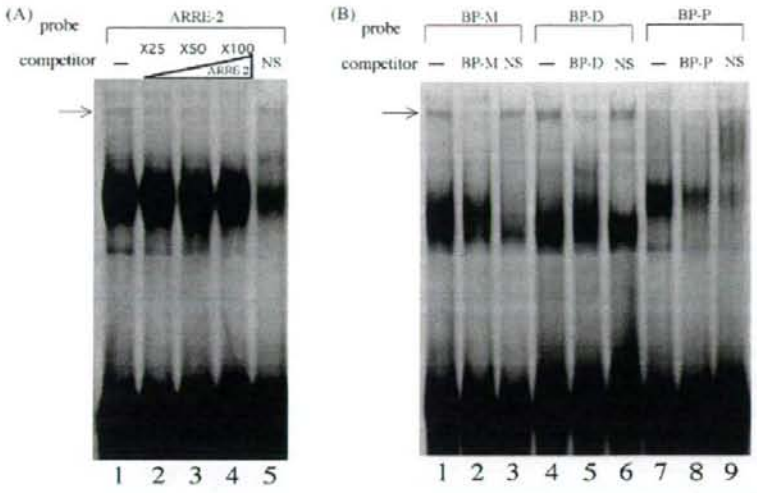

Fig. 4 Detection of NFAT binding activity in NHEK nuclear protein. Nuclear protein was extracted from NHEK cultured in KGM. (A) Electrophoretic gel mobility shift assays were performed using a double-stranded oligonucleotide DNA (5'-CGCCCAAAGAGGAAA ATTTGTTTCATA-3'), labeled with ^{32}P, that includes the NFAT consensus sequence (ARRE-2 site) of the promoter region of IL-2 gene. Arrow indicates specific binding of the ARRE-2 probe to NHEK nuclear protein, suggesting the existence of NFAT proteins. NS: non-specific sequence. (B) NFAT binding activity on BP-P, BP-M, and BP-D, which contain different NFAT consensus sequences identified in BPAG1 promoter region, was examined. As competitors, 100-fold excess of unlabeled probe itself (lanes 2, 5 and 8) or scrambled sequences (lanes 3, 6 and 9) were used. The arrow indicates specific NFAT binding activity to BP-M and BP-D probes.

Moreover, induction of NFAT-dependent transcription by activated Notch 1 was shown to be inhibited by treatment with CsA [5]. These findings together imply that CsA can modulate NFAT activity not only by inhibiting the nuclear translocation but also by reducing the NFAT expression.

BPAG1 gene, which is expressed prominently in the epidermal basal cell layer and disappears after initiation of differentiation of epidermal keratinocytes, was utilized as a reporter gene of undifferentiated keratinocytes [7,16]. We have previously reported that BPAG1 expression is downregulated by IFN-γ through direct transcriptional regulation [17]. Here, we demonstrate that BPAG1 gene expression is modulated by CsA. Specifically, (1) the CsA-responsive down-regulatory region is located within the 1.9-kb fragment of BPAG1 gene promoter; (2) three NFAT consensus sequences exist in this 1.9-kb region; (3) CsA in 10^{-6} and 10^{-7} concentrations significantly decreased BPAG1 gene promoter activity at 6- and 12-h points; and (4) specific binding activity to the BPAG1-NFAT sequences exists in keratinocyte nuclear protein, although supershift assay is further required to determine the NFAT isoform specifically bound to the NFAT consensus sequences in the BPAG1 promoter region. In this regard, calcineurin/NFAT activity has directly been implicated in keratinocyte growth/differentiation control [3–5] and in control of the hair cycle [6]. Taken together, the present study strongly suggests that calcineurin/NFAT system is directly involved in the control of epidermal keratinocyte gene expression, including BPAG1, and regulates epidermal differentiation. It should be noted that the down regulation of BPAG1 promoter activity was relatively transient. This may explain the small and partial reduction of BPAG1 mRNA levels by CsA. The present study demonstrated that the mRNA expression levels of involucrin, a marker of differentiated keratinocytes, were significantly decreased by CsA in consistent with the previous results in vivo [6]. In this regard, the gene expression of BPAG1, a marker of undifferentiated keratinocytes, is supposed to be upregulated by CsA. The mechanism of the paradoxical gene regulation by CsA of BPAG1 and involucrin shown in this study remains to be clarified.

Collectively, orchestration of cell fate might be controlled by calcineurin/NFAT system at transcriptional level in various cell types, including epidermal keratinocytes. Further elucidation of the details of this molecular mechanism in the regulation of growth and differentiation of epidermal keratinocytes by NFATs may allow development of novel therapeutic modalities for inflammatory and hyperproliferative skin diseases, such as psoriasis vulgaris.

Acknowledgments

The authors thank Carol Kelly and Eiko Soma for assistance.

References

[1] Rao A, Luo C, Hogan PG. Transcription factors of the NFAT family: regulation and function. Annu Rev Immunol 1997;15:707–47.

[2] Fisher GJ, Duell EA, Nickoloff BJ, Annesley TM, Kowalke JK, Ellis CN, et al. Levels of cyclosporin in epidermis of treated psoriasis patients differentially inhibit growth of keratinocytes cultured in serum free versus serum containing media. J Invest Dermatol 1988;91:142–6.

[3] Santini MP, Talora C, Seki T, Bolgan Loretta, Dotto P. Cross talk among calcineurin, Sp1/Sp3, and NFAT in control of p21WAF1/CIP1 expression in keratinocyte differentiation. Proc Natl Acad Sci USA 2001;98:9575–80.

[4] Al-Daraji WI, Grant KR, Ryan K, Saxton A, Reynolds NJ. Localization of calcineurin/NFAT in human skin and psoriasis and inhibition of calcineurin/NFAT activation in human keratinocytes by cyclosporin A. J Invest Dermatol 2002;118: 779–88.

[5] Mammucari C, di Vignano AT, Sharov AA, Neilson J, Havrda MC, Roop DR, et al. Integration of Notch 1 and calcineurin/NFAT signaling pathways in keratinocyte growth and differentiation control. Dev Cell 2005;8:665–76.

[6] Gafter-Gvili A, Sredni B, Gal R, Gafter U, Kalechman Y. Cyclosporin A-induced hair growth in mice is associated with inhibition of calcineurin-dependent activation of NFAT in follicular keratinocytes. Am J Physiol Cell Physiol 2003;284:C1593–603.

[7] Stanley JR, Hawley-Nelson P, Yuspa SH, Shevach EM, Katz SI. Characterization of bullous pemphigoid antigen: a unique basement membrane protein of stratified squamous epithelia. Cell 1981;24:897–903.

[8] Gregersen JW, Holmes S, Fugger L. Humanized animal models for autoimmune diseases. Tissue Antigens 2004;63:282–394.

[9] Tamai K, Sawamura D, Do HC, Tamai Y, Li K, Uitto J. The human 230-kDa bullous pemphigoid antigen gene (BPAG1). Exon-intron organization and identification of regulatory tissue specific elements in the promoter region. J Clin Invest 1993;92:814–22.

[10] Andrews NC, Faller DV. A rapid micropreparation technique for extraction of DNA-binding proteins from limiting numbers of mammalians cells. Nucleic Acids Res 1991;19: 2499.

[11] Vindevoghel L, Chung KY, Davis A, Kouba D, Kivirikko S, Alder H, et al. A GT-rich sequence binding the transcription factor Sp1 is crucial for high expression of the human type VII collagen gene (COL7A1) in fibroblasts and keratinocytes. J Biol Chem 1997;272:10196–204.

[12] Park J, Takeuchi A, Sharma S. Characterization of a new isoform of the NFAT (nuclear factor of activated T cells) gene family member NFATc. J Biol Chem 1996;34:29014–21.

[13] Lopez-Rodriguez C, Aramburu J, Rakeman AS, Rao A. NFAT5, a constitutively nuclear NFAT protein that does not cooperate with Fos and Jun. Proc Natl Acad Sci USA 1999;99: 7214–9.

[14] McCaffrey PG, Perrino BA, Soderling TR, Rao A. NF-ATp, a T lymphocyte DNA-binding protein that is a target for calcineurin and immunosuppressive drugs. J Biol Chem 1993;15: 3747–52.

[15] Macian F, Garcia-Rodriguez C, Rao A. Gene expression elicited by NFAT in the presence or absence of cooperative recruitment of Fos and Jun. EMBO J 2000;19:4783–95.

[16] Tamai K, Silos SA, Li K, Korkeela E, Ishikawa H, Uitto J. Tissue-specific expression of the 230-kDa bullous pemphigoid antigen gene (BPAG1). Identification of a novel keratinocyte regulatory *cis*-element KRE3. J Biol Chem 1995;270: 7609–14.

[17] Tamai K, Li K, Silos S, Rudnicka L, Hashimoto T, Nishikawa T, et al. Interferon-gamma-mediated inactivation of transcription of the 230-kDa bullous pemphigoid antigen gene (BPAG1) provides novel insight into keratinocyte differentiation. J Biol Chem 1995;270:392–6.

Uncorrected Version. Published on August 7, 2008 as DOI:10.2353/ajpath.2008.070977

The American Journal of Pathology, Vol. 173, No. 3, September 2008

DOI: 10.2353/ajpath.2008.070977

Bone Marrow Cell Transfer into Fetal Circulation Can Ameliorate Genetic Skin Diseases by Providing Fibroblasts to the Skin and Inducing Immune Tolerance

Takenao Chino,*† Katsuto Tamai,* Takehiko Yamazaki,* Satoru Otsuru,* Yasushi Kikuchi,* Keisuke Nimura,* Masayuki Endo,* Miki Nagai,† Jouni Uitto,‡ Yasuo Kitajima,† and Yasufumi Kaneda*

From the Division of Gene Therapy Science, Osaka University Graduate School of Medicine, Osaka, Japan; the Department of Dermatology,† Gifu University School of Medicine, Gifu, Japan; and the Department of Dermatology and Cutaneous Biology,‡ Jefferson Medical College, Thomas Jefferson University, Philadelphia, Pennsylvania*

Recent studies have shown that skin injury recruits bone marrow-derived fibroblasts (BMDFs) to the site of injury to accelerate tissue repair. However, whether uninjured skin can recruit BMDFs to maintain skin homeostasis remains uncertain. Here, we investigated the appearance of BMDFs in normal mouse skin after embryonic bone marrow cell transplantation (E-BMT) with green fluorescent protein-transgenic bone marrow cells (GFP-BMCs) via the vitelline vein, which traverses the uterine wall and is connected to the fetal circulation. At 12 weeks of age, mice treated with E-BMT were observed to have successful engraftment of GFP-BMCs in hematopoietic tissues accompanied by induction of immune tolerance against GFP. We then investigated BMDFs in the skin of the same mice without prior injury and found that a significant number of BMDFs, which generate matrix proteins both *in vitro* and *in vivo*, were recruited and maintained after birth. Next, we performed E-BMT in a dystrophic epidermolysis bullosa mouse model (col7a1$^{-/-}$) lacking type VII collagen in the cutaneous basement membrane zone. E-BMT significantly ameliorated the severity of the dystrophic epidermolysis bullosa phenotype in neonatal mice. Type VII collagen was deposited primarily in the follicular basement membrane zone in the vicinity of the BMDFs. Thus, gene therapy using E-BMT into the fetal circulation may offer a potential treatment option to ameliorate genetic skin diseases that are characterized by fibroblast dysfunction through the introduction of immune-tolerated BMDFs. *(Am J Pathol 2008, 173:803–814; DOI: 10.2353/ajpath.2008.070977)*

Bone marrow (BM) has been shown to harbor progenitor cells of bone marrow-derived fibroblasts (BMDFs) that have the propensity to migrate into injured tissues, including the skin.[1–7] Previous studies have shown that wounded skin recruits BMDFs that become resident cells and accelerate tissue repair and wound-healing processes.[8,9] However, whether BMDFs can contribute to healthy skin without prior injury to maintain homeostasis of the structure and function remains unclear, in part because marker gene-transgenic bone marrow transplantation (BMT) for tracing the fate of the transplanted cells in mice requires lethal doses of irradiation that injures all tissues including the skin. Consequently, we have now investigated the fate of the transplanted bone marrow cells (BMCs) in the skin under physiological conditions without irradiation and injury.

Embryonic transplantation of congenic, and possibly allogenic, BMCs transduced with a marker gene, such as green fluorescent protein (GFP), in animal models showed that the transplanted cells successfully engrafted in the recipient BM for long periods without prior myeloablative regimen, such as lethal irradiation, and generated hematopoietic chimerism by inducing immune tolerance.[10] In this context, embryonic-BMT (E-BMT) might allow us to evaluate the potency of BM to raise

Supported by health science research grants for research on specific disease from the Ministry of Health, Labor, and Welfare of Japan; by grants-in-aid for scientific research from the Ministry of Education, Culture, Sports, Science, and Technology of Japan; and by the National Institutes of Health, U.S.A.

Accepted for publication May 29, 2008.

Supplemental material for this article can be found on *http://ajp.amjpathol.org*.

Address reprint requests to Katsuto Tamai, M.D., Ph.D., or Yasufumi Kaneda, M.D., Ph.D., Division of Gene Therapy Science, Osaka University Graduate School of Medicine, 2-2 Yamadaoka, Suita, Osaka 565-0871, Japan. E-mail: tamai@gts.med.osaka-u.ac.jp, and kaneday@gts.med.osaka-u.ac.jp.

BMDFs in normal skin without injury. However, previous E-BMT mouse protocols are rather invasive to the embryo with a high incidence of embryonic death. Furthermore, there is a limitation to the number of cells for transplantation because such E-BMT procedures require direct injection of the BMCs into the fetus by intraperitoneal, subcutaneous, or intrahepatic approaches.[11]

Recently, a far less invasive E-BMT via the vitelline vein, which is located under the uterine wall and directly communicates with the embryonic circulation, was shown to generate efficient hematopoietic chimerism.[12] Because this E-BMT procedure allows the transfer of as many as 1.0×10^6 cells/embryo without embryonic tissue damage, we can trace the fate of the transplanted GFP-transgenic bone marrow cells (GFP-BMCs) in the hematopoietic and nonhematopoietic tissues of the mice undergoing physiological development during the fetal and postnatal periods.

Clinically, E-BMT via fetal circulation has been applied to human hematopoietic and enzyme storage diseases, such as severe combined immunodeficiency (SCID) and leukodystrophy, to provide functional hematopoietic lineage of cells in conjunction with inducing immune tolerance against the transplanted allogenic cells.[13] For nonhematopoietic tissue diseases, however, the therapeutic potential of E-BMT has not been well established. If E-BMT can generate a significant number of immunologically tolerated allogenic BMDFs that synthesize matrix molecules, such as collagen, in the skin after birth, it may provide a therapeutic option for inherited skin diseases with defective matrix molecules attributable to genetic fibroblast dysfunction.

Dystrophic epidermolysis bullosa (DEB) is a family of inherited mechanobullous skin disorders caused by mutations in the COL7A1 gene that encodes type VII collagen necessary for stable epidermal-dermal adherence.[14–16] Previous studies have suggested that both epidermal keratinocytes and dermal fibroblasts are capable of synthesizing type VII collagen.[17–19] It was then demonstrated that transplanted dermal fibroblasts were capable of producing type VII collagen at the cutaneous basement membrane zone.[20,21] Another study showed that type VII collagen-transgenic fibroblasts supplied type VII collagen to the dermal-epidermal junction more efficiently than gene-transgenic keratinocytes.[22] More recently, Wong and colleagues[23] demonstrated the clinical potential of allogenic fibroblast cell therapy for recessive DEB (RDEB) patients. These studies suggest that transplantation of functional fibroblasts may be a promising therapeutic option for DEB treatment.[24]

In case of the most severe, so-called Hallopeau-Siemens type of RDEB (HS-RDEB), the patients frequently harbor nonsense mutations in both alleles of COL7A1 and demonstrate no expression of the corresponding gene, leading to the suggestion that HS-RDEB patients might not have immune tolerance against type VII collagen molecules if introduced by gene therapy. If this is indeed the case, therapies with allogenic fibroblasts or recombinant type VII collagen may result in failure because of antibody formation and immunological rejection. To overcome such difficulties, E-BMT may be an ideal procedure for this disease, not only by providing functional BMDFs but also inducing immune tolerance against allogenic BMDFs expressing type VII collagen.

In this study, we searched for evidence of BMDF generation in normal mouse skin after E-BMT with congenic GFP-BMCs via the vitelline vein. We also evaluated immune tolerance induction against an exogenously introduced non-self molecule, GFP, by E-BMT with the GFP-BMCs. Finally, we investigated the therapeutic potential of E-BMT to DEB model mice, which ordinarily die within a few days after birth because of skin separation. We succeeded in showing, for the first time, that E-BMT could be a therapeutic option for DEB by providing type VII collagen molecules from functional BMDFs.

Materials and Methods

Mouse Recipients and Donors

Day 12 to 13 embryos of C57BL/6 mice were BMT recipients, and GFP-transgenic C57BL/6 donor mice were kindly provided by Dr. M. Okabe (Osaka University, Osaka, Japan).

Preparation of Donor BMCs

Adult GFP$^+$ BMCs (GFP-BMCs) were isolated from GFP-transgenic mice (C57BL/6 background) 8 weeks after birth by flushing the tibiae and femurs with RPMI 1640 medium (Nacalai Tesque, Kyoto, Japan) containing 10% fetal bovine serum using a 27-gauge needle. After filtration through a 40-μm nylon mesh filter, GFP-BMCs were centrifuged at 440 $\times$ *g* for 7 minutes at 24°C. CD90$^+$ T cells were magnetically depleted by negative selection with anti-CD90 (Miltenyi Biotec, Gladbach, Germany). The GFP-BMCs were counted and suspended in Ca/Mg-free phosphate-buffered saline (PBS; Nacalai Tesque) at a density of 1.0×10^8 cells/ml for injection.

Embryonic BMC Transplantation via the Vitelline Vein

Embryonic BMC transplantation via the vitelline vein was performed as described previously.[10] Briefly, pregnant mice (C57BL/6) on days 12 to 13 of gestation were anesthetized, and the uterus was exposed through a midline laparotomy incision under sterile conditions. Beveled glass micropipettes were placed under stereoscopic microscopy into the vitelline vein (Figure 1A), which directly communicates with the fetus *in utero*. Each injection contained 1.0×10^6 viable GFP-BMCs in 10 to 20 μl of PBS. In the case of the DEB model mice, each injection contained 0.5×10^6 viable GFP-BMCs in 10 to 20 μl of PBS. For an unknown reason, all embryos of the DEB model mice died when more than 0.5×10^6 viable GFP-BMCs was injected. The uterus and fetus were returned to the abdomen, which was closed using a 4–0 silk suture. For each pregnancy, GFP-BMCs were injected on the average into seven fetuses via the vitelline vein within 1 hour.

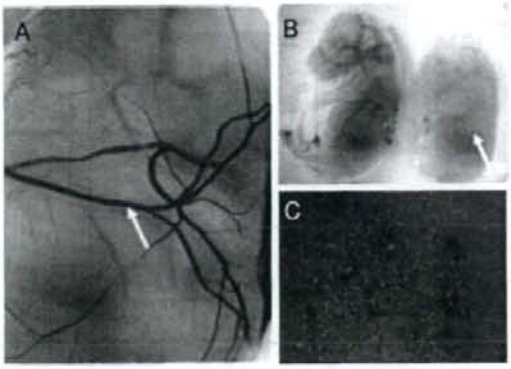

Figure 1. Successful delivery of BMCs to mouse embryos via the vitelline vein. **A:** Vitelline vein (**arrow**) of a day E13 embryo in amnion under stereoscopic microscope observation. **B:** Successful injection of toluidine blue-containing solution via the vitelline vein at day E13 (**right, white arrow, left, an uninjected control**). **C:** Day E13 mouse skin at 30 minutes after GFP-transgenic E-BMT via the vitelline vein. Original magnification, ×80.

The uterus was frequently flooded with warm sterile saline during the procedure to prevent drying and to maintain the maternal temperature.

Fluorescence Stereoscopic Microscopy

All of the mouse organs at 11 to 12 weeks after the embryonic GFP-BMT were directly observed under a microscope equipped with a mercury lamp (Leica Microsystems AG, Wetzlar, Germany) and GFP filters.

Analysis of Bone Marrow Chimerism

Recipients of GFP-BMT were euthanized between 2 to 6 months after embryonic BMT and the BMCs were harvested by flushing the tibiae and femurs with PBS using a 28-gauge needle. After passage through a 40-μm nylon mesh filter, the red blood cells were lysed for 1 to 2 minutes using ACK lysing buffer (Cambrex Bio Science, Walkersville, MD). Samples were analyzed using a FACScan (Becton Dickinson, San Diego, CA).

Skin Grafting

Full thickness tail skin from transgenic GFP mice isolated by excision under anesthesia was cut into ~10 × 10-mm squares. The GFP-positive tail skin was engrafted onto the back of recipient mice at 6 weeks after birth just above the muscular fascia and secured with a bandage for 7 days.

Measurement of Antibody Generation against GFP

Tail skin of GFP mice was engrafted onto the back of 6-week-old mice after E-BMT or neonatal subcutaneous transplantation with 1.0×10^6 of GFP-BMCs, GFP fibroblasts, or GFP mesenchymal stem cells above the muscular fascia, and secured with a bandage for 7 days. At 4 weeks after GFP skin engraftment, blood samples were collected from tail snips, pooled, and stored at −20°C. Recombinant GFP was diluted to a working concentration of 0.2 μg/ml in PBS, and 96-well microtiter plates were coated with 100 μl per well and incubated at 4°C overnight. The plates were rinsed twice with washing buffer (0.05% Tween 20 in PBS), and 200 μl of blocking buffer (2% skim milk in PBS) was then added to each well, and the plates were incubated for 2 hours. The antibody harvested from the mice engrafted with GFP skin was diluted 1:250 in PBS, and 100 μl per well was added for 1 hour at room temperature. After rinsing with washing buffer, 100 μl of secondary antibody (anti-mouse IgG, horseradish peroxidase) was added to each well for 1 hour. The microplates were washed and the levels of antibody generated against GFP were measured.

Cytotoxic T-Cell (CTL) Assay against GFP

Mice were anesthetized and splenocytes harvested from isolated spleens by passage through a sterile strainer. The splenocytes were then sedimented by centrifugation at 450 × *g* for 10 minutes and red blood cells were depleted using ACK buffer for 1 to 2 minutes. The GFP-BMCs from GFP-transgenic mice 8 weeks after birth were harvested, sedimented by centrifugation at 440 × *g* for 7 minutes at room temperature, resuspended in RPMI 1640, and incubated with Mitomycin C (Nacalai Tesque) for 45 minutes. Finally, isolated splenocytes (5×10^7/ml) were co-cultured with GFP-BMCs (5×10^6/ml) in 75-cm^2 BD Falcon dishes (BD Biosciences, San Jose, CA) with rhIL-2 at 37°C. After sensitization with the simulator GFP-BMCs for 7 days, the effector splenocytes were harvested and portioned into 96-well tissue culture plates. Responder GFP-BMCs from GFP-transgenic mice were cultured with ^{51}Cr (Amersham BioSciences UK, Ltd., Buckinghamshire, UK) for 30 minutes and mixed with the effector splenocytes for 4 hours. The release of ^{51}Cr from GFP-BMCs disrupted by splenocyte CTL activity into the supernatant was determined by scintillation counting.

Immunofluorescence Analysis

Embryonic BMT mice were fixed by perfusion with 4% paraformaldehyde under anesthesia. The skin tissues were soaked overnight in 4% paraformaldehyde and embedded in Tissue-Tek OCT compound (Sakura Finetek Japan, Tokyo, Japan). The tissues were frozen in liquid nitrogen and stored at −20°C. Sections (6 μm) were cut on a cryostat (Leica Microsystems AG) and fixed in 4% paraformaldehyde for 10 minutes at room temperature. The sections were reacted with rabbit polyclonal anti-mouse type I collagen (1:100), anti-mouse fibronectin (1:100), anti-mouse vimentin (1:100), and anti-mouse type VII collagen (1:200) antibodies, followed by the secondary antibody, Alexa Fluor 546 goat anti-rabbit IgG (1:200, Molecular Probes, Eugene, OR). The sections were finally stained with 4,6-diamidine-2-phenylindole dihydrochloride, mounted with the antifade solution, Vector

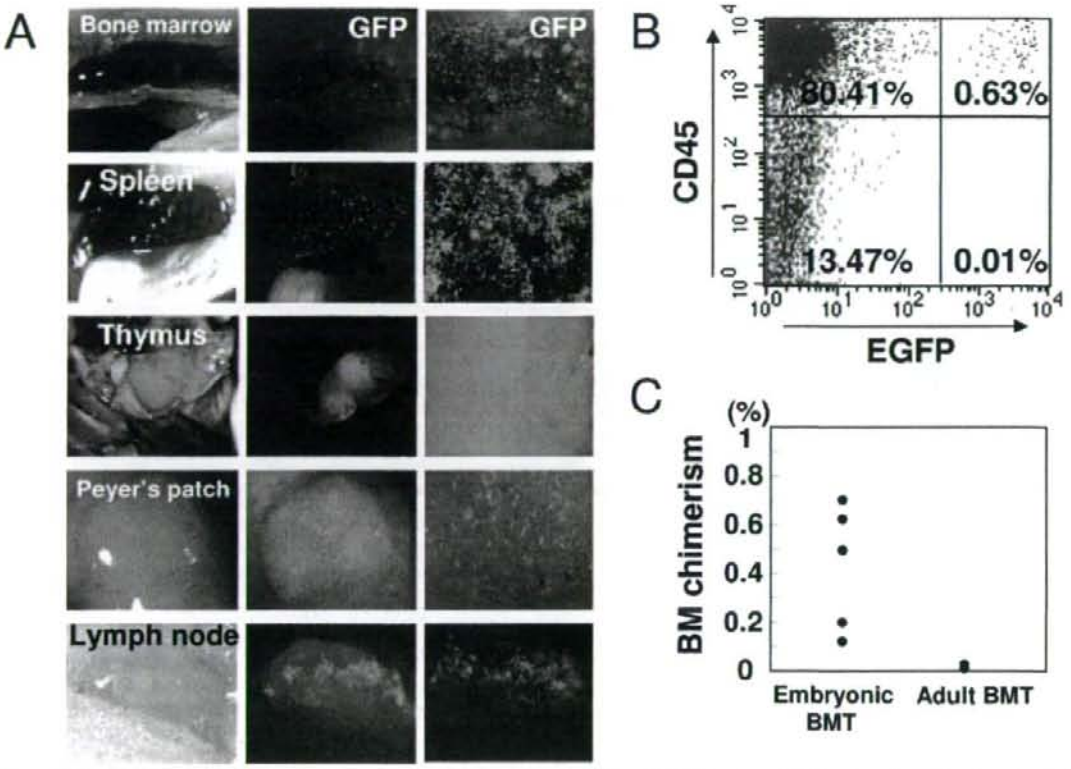

Figure 2. Hematopoietic tissues containing GFP$^+$ cells after embryonic BMT. **A:** GFP$^+$ cells from GFP$^+$ BM are located in BM, spleen, thymus, Peyer's patches, and lymph nodes at 13 weeks after embryonic GFP-BMT. Original magnifications: ×40 (**A, middle**); ×80 (**A, right**). **B:** FACS analysis of BMCs harvested at 12 weeks after embryonic BMT. GFP$^+$ cells in BM account for 0.63% of all cells, and more than 99.9% of GFP$^+$ BMCs co-express CD45. **C:** Chimerism of GFP$^+$ BMCs in each transplantation. The relative amount (%) of donor cells in BM measured by FACScan is shown. Each point represents the degree of engraftment in BM in embryonic ($n = 5$) and adult ($n = 5$) GFP-BMT mice. The percentage of GFP$^+$ cells varies between 0.1% and 0.7% of all cells according to FACS analysis of BMCs from adult mice with embryonic BMT (**left column**). No engraftment of GFP$^+$ cells is evident in nonirradiated 8-week-old adult mice with GFP-BMT (**right column**).

Shield (Vector Laboratories, Inc., Burlingame, CA) and covered with a coverslip.

Isolation of Bone Marrow-Derived GFP$^+$ Cells from the Dermis of E-BMT Mice

The BM-derived GFP$^+$ cells were isolated from the dermis of E-BMT mice at more than 12 weeks of age. Full thickness skin ~10 × 10 mm, was isolated from BMT mice isolated by excision under systemic anesthesia, and treated with 1000 PU/ml dispase for 30 minutes at 37°C to separate the epidermis from the dermis. The dermal sheets were then cut into ~1 mm squares, incubated for 45 minutes in medium containing bacterial collagenase (Yakult Pharmaceutical Inc., Tokyo, Japan) at 37°C until the skin was visibly dissociated. The cell suspension was grown in Minimal Essential Medium supplemented with 10% fetal bovine serum for 2 to 3 days. The cells were then harvested by trypsinization for 10 minutes and sorted into GFP$^+$ cells and GFP$^-$ cells with FACScan (Becton Dickinson) using CellQuest software.

RNA Extraction and Reverse Transcriptase-Polymerase Chain Reaction (RT-PCR) Analysis

Total RNA was extracted from GFP$^+$ BMCs, GFP$^+$ fibroblasts, and sorted BM-derived GFP$^+$ cells using a RNeasy mini kit (Qiagen, Valencia, CA); 5 μg of total RNA was reverse-transcribed into the first strand cDNA in a reaction primed by random hexamers primer using Superscript 3 reverse transcriptase (Invitrogen Corp., Carlsbad, CA). First strand cDNA was used as template for PCR reactions using Taq polymerase (Takara Pharmaceutical Inc., Ostu, Japan).

Primers used were as follows: fibronectin: 5′-GAGACAGCCGTGACCCAGACTTA-3′ (forward); 5′-CTTCTTTCCAGCGACCCGTAGAG-3′ (reverse), 30 cycles, product size 940 bp; collagen-1: 5′-CTACTCAGCCGTCTGTGCCT-3′ (forward); 5′-GGCAGGGCCAATGTCTAGT-3′ (reverse), 30 cycles, product size 450 bp; procollagen 1α-1: 5′-CCCAGTGGCGGTTATGACTT-3′ (forward); 5′-TGAGGCACAGACGGCTGAGTA-3′ (reverse), 30 cycles, product size 353 bp; DDR2: 5′-AACCCGATGACCTGAAGGAA-3′

(forward); 5′-CTGGGATAAGGCGAACAAAT-3′ (reverse), 30 cycles, product size 270 bp; type 7 collagen: 5′-CTCT-TGGCCCCCGAGGAAGAG-3′ (forward); 5′-GTCCTCGG-GGACCTTCTT G-3′ (reverse), 30 cycles, product size 320 bp; GFP: 5′-CTACAAGACCCGCGCCGAGGTGAAG-3′ (forward); 5′-GTGACCGCCGCCGGGATCACTC-3′ (reverse), 30 cycles, product size 376 bp; GAPDH: 5′-TTGAAGGTAGTT-TCGTGGAT-3′ (forward); 5′-GAAAATCTGGCACCACAC-CTT-3′ (reverse), 30 cycles, product size 265 bp. Reactions were cycled at 95°C for 30 seconds [58°C (fibronectin), 55°C (collagen 1, procollagen 1α-1, type 7 collagen, GFP, GAPDH), 52°C (DDR2)] for 30 seconds, and 72°C for 1 minute. mRNA transcript-specific amplification products were separated electrophoretically on a 1% agarose gel using All-Purpose Hi-Lo DNA marker (Bionexus Inc., Oakland, CA) for the determination of the amplicon size.

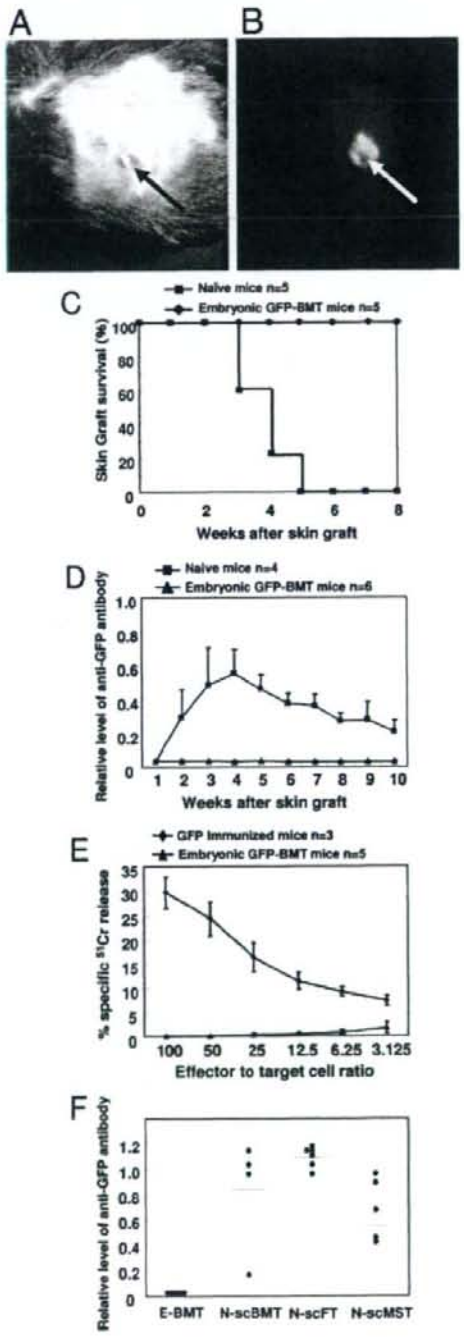

Electron Microscopic Analysis

Skin specimens were fixed with 2% glutaraldehyde in 0.1 mol/L sodium phosphate buffer, pH 7.4, for 5 to 7 minutes at 37°C, followed by fixation with a 2% aqueous solution of osmium tetroxide (OsO4) for 4 hours at 37°C. Fixed samples were embedded in Epon 812 (Nisshin EM Company, Ltd., Tokyo, Japan). Ultrathin sections were made parallel to the bottom of the dish and counterstained with uranyl acetate and lead citrate. From some specimens, 4 to 5 serial thin sections (100 nm thick) were made and subjected to standard transmission electron microscopic examination.

Results

E-BMT via the Vitelline Vein Efficiently Distributes Donor Cells to the Fetus

To ensure the effective transfer of transplanted BMCs into fetal circulation, GFP-BMCs were introduced via the vitelline vein, which directly communicates with the fetal circulation, at embryonic day 13 (Figure 1A). In some

Figure 3. Engraftment of GFP-transgenic skin on embryonic GFP-BMT mice and evaluation of humoral and cellular immunity against GFP. **A** and **B:** Skin from GFP-transgenic mouse tail is engrafted 7 weeks after embryonic GFP-BMT. Engrafted GFP transgenic skin under normal (**A**, **black arrow**) and GFP fluorescent (**B**, **white arrow**) light. The engrafted GFP-transgenic skin persisted for more than 50 weeks. **C:** Skin graft survival. Survival of GFP skin graft at 6 weeks in embryonic BMT ($n = 5$) and naïve ($n = 5$) mice. Engrafted skin persisted beyond 8 weeks after grafting in all mice that had undergone embryonic BMT. All skin grafts were rejected by nonirradiated adult naïve mice before 5 weeks after grafting. **D:** Generation of antibodies against GFP. Antibodies against GFP in transplanted skin were measured using ELISA. Naïve mice ($n = 4$) produced significant amounts of antibodies (mean + SE), whereas embryonic GFP-BMT mice ($n = 6$) did not. **E:** Cytotoxic T-cell (CTL) assay against GFP measured in embryonic GFP-BMT mice ($n = 5$) and GFP-immunized mice ($n = 3$) in response to GFP$^+$ BMCs. Assays were performed in triplicate (mean ± SE). Embryonic mice with GFP-BMT generated no response whereas those with GFP generated significant responses. **F:** Generation of antibodies against GFP. Antibody titers against GFP in the mouse serum after transplantation of GFP-transgenic skin were measured using ELISA. Subcutaneous transplantation of GFP-BMCs (N-scBMT, $n = 4$), GFP-fibroblasts (N-scFT, $n = 7$), and GFP-mesenchymal stem cells (N-scMST, $n = 5$) in neonatal mice did not prevent these mice from generating anti-GFP antibodies after GFP skin transplantation, whereas embryonic GFP-BMT mice (E-BMT, $n = 6$) did not develop anti-GFP antibodies.

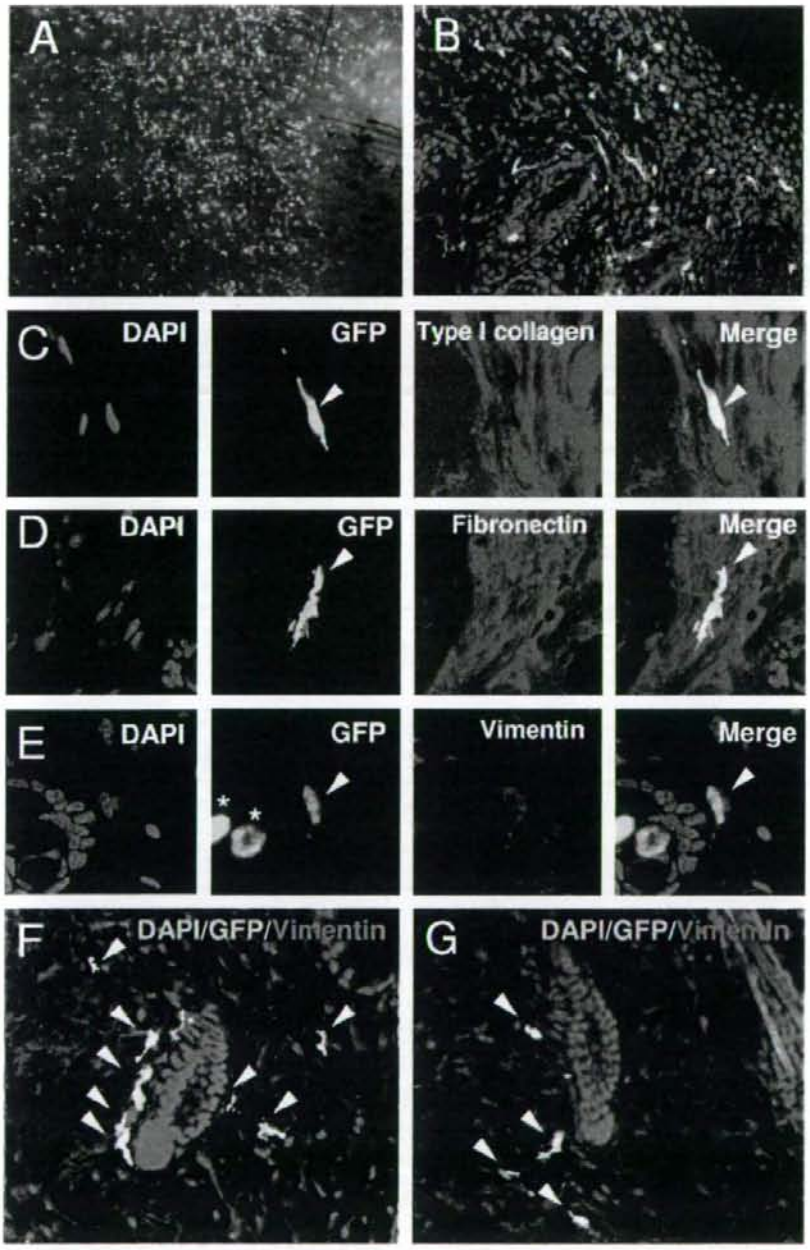

Figure 4. Generation of BMDFs by E-BMT in normal skin. **A:** Confocal microscopic picture of adult mouse skin at 13 weeks after GFP-transgenic E-BMT (12 weeks after birth). Note that a significant number of GFP-transgenic BMCs provided by the E-BMT appear scattered on the skin. **B:** Transplanted GFP$^+$ BM-derived cells in the adult mouse skin with E-BMT. The majority of the GFP$^+$ BM-derived cells resided within the dermal matrix. **C–E:** GFP$^+$ BM-derived cells (**white arrowheads**) were stained with fibroblast marker proteins, including type I collagen (**C**), fibronectin (**D**), and vimentin (**E**). **E:** **Asterisks** indicate autofluorescence of the hair shafts. **F** and **G:** Most of GFP$^+$ BM-derived cells (**white arrowhead**) were stained with fibroblastic marker proteins including vimentin around hair follicles. Original magnifications: ×40 (**A**); ×100 (**B**); ×400 (**C–E**); ×200 (**F**, **G**).

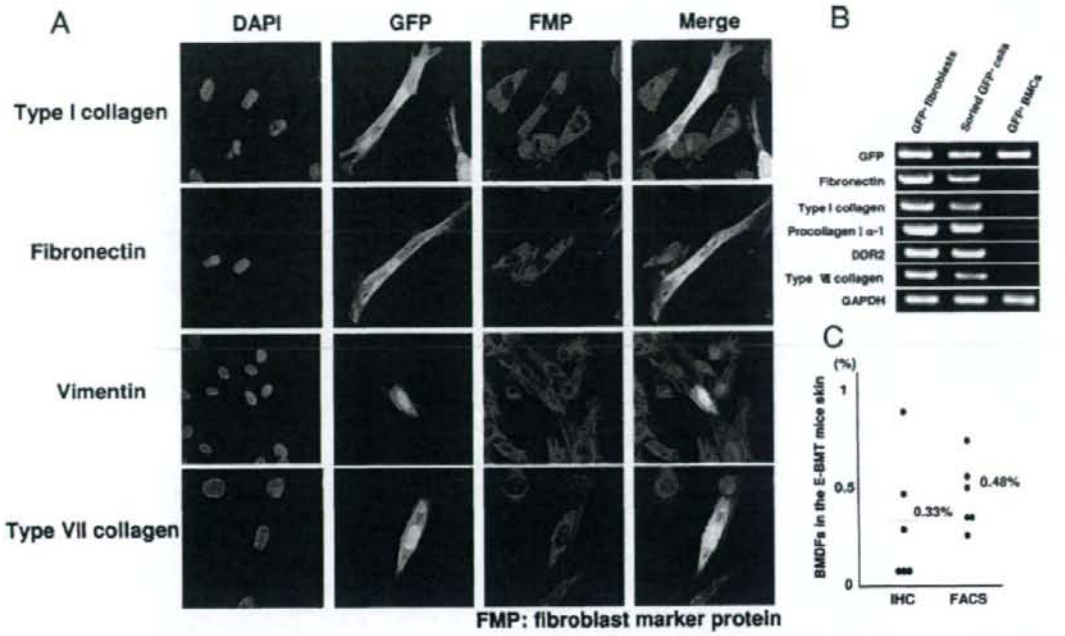

Figure 5. Characterization of BMDFs in culture. **A:** Immunostaining of the cultured fibroblasts from the adult mouse skin with E-BMT for fibroblastic marker proteins. Note that GFP$^+$ BMDFs express fibroblast marker proteins including type I collagen, fibronectin, vimentin, and type VII collagen. **B:** RT-PCR analysis of the sorted BMDFs from the cultured fibroblasts derived from the skin of adult mice with E-BMT. Both the GFP$^+$ BMDFs and the fibroblasts from GFP-transgenic mouse skin expressed fibroblast marker genes including fibronectin, type I collagen, procollagen I-α, DDR2, and type VII collagen as well as GAPDH. Note that BMCs of the GFP-transgenic mouse did not express any of those genes except GAPDH. **C:** FACS analysis for percentage of BMDFs in cultured dermal fibroblasts derived from wild-type mice (12 weeks old) with E-BMT (E-BMT, $n = 6$), and immunohistological evaluation for percentage of GFP-positive/vimentin-positive cells in total vimentin-positive cells in the dermis of the wild-type mouse (12 weeks old) with E-BMT in the skin specimens (IHS, $n = 6$). Original magnifications, ×400 (**A**).

experiments, toluidine blue dye was added to the suspension of GFP-BMCs, allowing us to monitor successful E-BMT by blue color staining of the embryonic skin (Figure 1B). Within 30 minutes after E-BMT, successful distribution of the transplanted BMCs to the fetal skin was confirmed by observing GFP$^+$ cells on the surface of the fetal skin by fluorescence stereoscopic microscopy as well as visual observation of blue color (Figure 1C).

Successful Engraftment of the GFP-BMCs in Hematopoietic Tissues of Mice with E-BMT

Successful long-term engraftment of the GFP-BMCs by E-BMT was confirmed by demonstration of hematopoietic chimerism of the donor and recipient cells in the BM and other hematopoietic tissues at 12 weeks after birth. Specifically, hematopoietic tissues, including BM, spleen, thymus, Peyer's patch, and lymph nodes, were shown to have an engraftment of cells derived from GFP-BMCs (Figure 2A). Fluorescence-activated cell sorting (FACS) analysis indicated that CD45$^+$ hematopoietic cells derived from E-BMT accounted between 0.1% and 0.7% of the total BMC population after a single-dose of E-BMT with 1.0×10^6 GFP-BMCs in five individual mice (Figure 2, A–C). On the other hand, no GFP-BMCs were detected at 12 weeks after BMT with GFP-BMCs in adult mice (Figure 2C). These findings suggest induction of immune tolerance against GFP protein by E-BMT.

Humoral and Cellular Immune Tolerance Induction against GFP by E-BMT

Previous studies have indicated that GFP protein is an intolerable immunogenic antigen that evokes both cellular and humoral immune response.[25] We then evaluated whether E-BMT of congenic GFP-BMCs can induce immune tolerance against GFP. First, E-BMT mice with 1.0×10^6 of congenic GFP-BMCs were transplanted with the skin from a congenic GFP-transgenic mouse (C57BL/6 background). Successful engraftment of the transplanted GFP-containing mouse skin was observed in all mice with E-BMT (Figure 3A–C), whereas the transplanted skin was rejected within 5 weeks after engraftment in all recipient mice without E-BMT (Figure 3C). Induction of anti-GFP antibodies, which was observed in all naïve mice with GFP skin transplantation, was completely inhibited by E-BMT (Figure 3D). Furthermore, cytotoxic immune reactivity of the thymic cells against cells harboring GFP was not detected by ^{51}Cr release assay in E-BMT mice (Figure 3E). These data clearly demonstrate that E-BMT in fetal mice with congenic GFP-BMCs is sufficient to induce both humoral and cellular immune

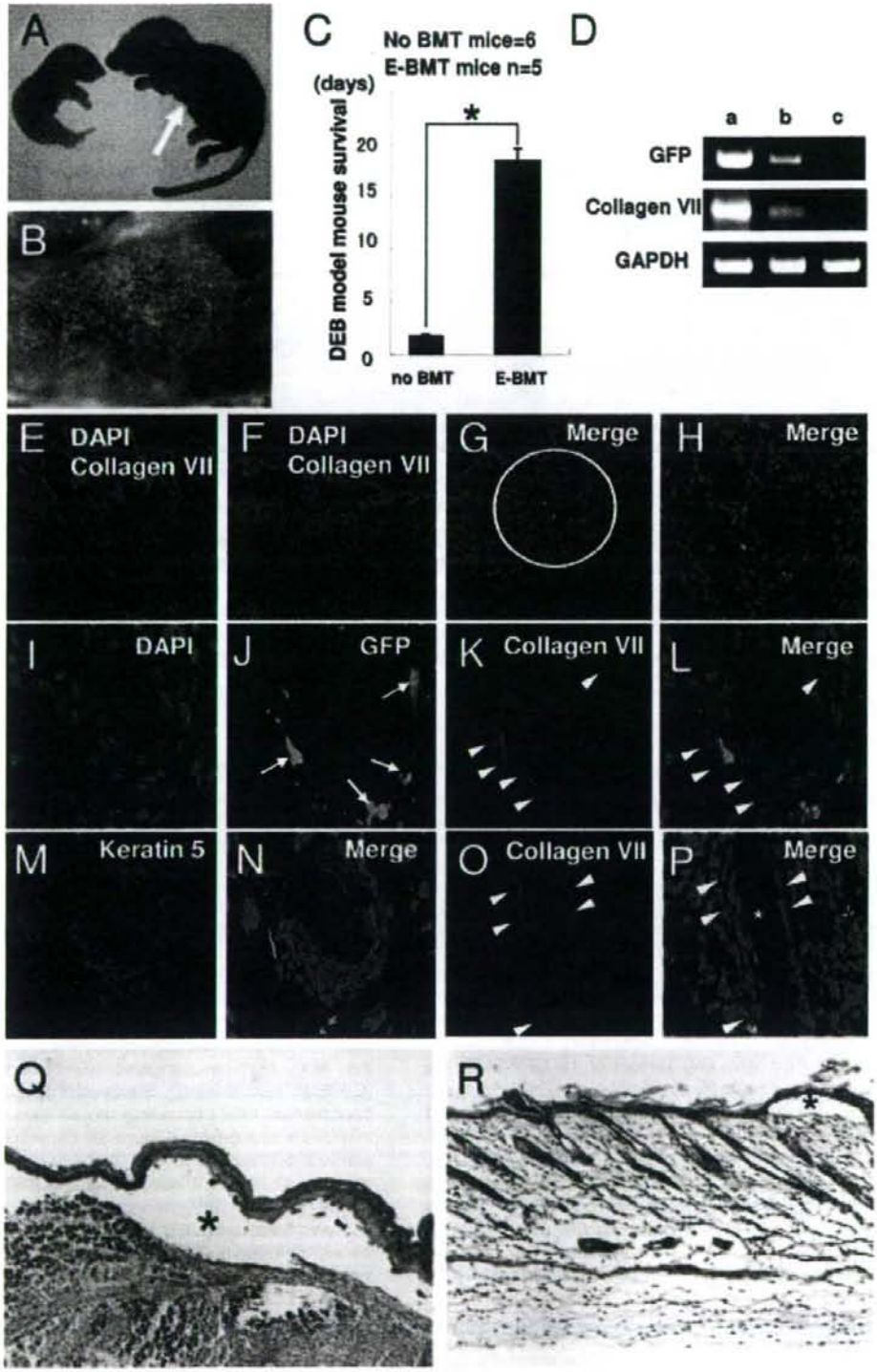

tolerance against GFP. Secondly, we compared the potential for immune tolerance induction against GFP between E-BMT and neonatal subcutaneous transplantation with various GFP-expressing cells, such as BMCs, fibroblasts, and mesenchymal stem cells. None of these cells could induce immune tolerance against GFP by postnatal subcutaneous transplantation, subsequently resulting in immunological rejection of the transplanted GFP mouse skin (data not shown), as well as in raising anti-GFP antibodies (Figure 3F).

Skin-Homing BMCs Provide BMDFs in Uninjured Skin after Birth

Next, we searched for evidence of BMDFs in the skin of E-BMT mice after birth. Fluorescence stereoscopic microscopy examination showed that numerous GFP$^+$ cells were dispersed over the entire skin of 12-week-old mice with E-BMT (Figure 4A). These GFP$^+$ cells were scattered within the dermal structures, as shown in histological sections of the skin (Figure 4B). We then examined the expression of fibroblast marker proteins on the transplanted BMC-derived cells in the skin of 12-week-old mice with E-BMT. Immunohistochemical examination revealed that some of the GFP$^+$ cells showed overlapping staining with antibodies against type I collagen (Figure 4C), fibronectin (Figure 4D), and vimentin (Figure 4, E–G). The GFP$^+$ cells expressing fibroblast marker proteins were intermingled with GFP$^-$ fibroblasts particularly around hair follicle structures in the skin (Figure 4, F and G), but less in the region of the dermo-epidermal junction (see Supplemental Figure S1 at *http://ajp.amjpathol.org*).

To characterize the GFP$^+$ cells expressing fibroblast marker proteins, dermal fibroblasts of the skin of 12-week-old mice with E-BMT were cultured. The GFP$^+$ cells were morphologically indistinguishable from GFP$^-$ fibroblasts in culture (Figure 5A). Immunofluorescent staining clearly showed that the cultured GFP$^+$ cells also expressed fibroblast marker proteins, including type I collagen, fibronectin, vimentin, and type VII collagen (Figure 5A).

After isolation of a pure GFP-positive population of cultured cells by a fluorescence-activated cell sorter (FACS), mRNA expression profiles for fibroblast markers of the sorted GFP$^+$ cells were compared with fibroblasts and BMCs obtained from GFP-transgenic mice by RT-PCR. Identical profiles of the mRNA expression were observed between fibroblasts and the sorted GFP$^+$ cells, whereas BMCs did not show any mRNA expression of the fibroblast marker genes (Figure 5B). Quantitative analysis of the sorted GFP$^+$ fibroblasts showed that ~0.5% of the cells were BMDFs in cultures of fibroblasts from six different mice with E-BMT (Figure 5C). In addition, we evaluated the percentage of the GFP-positive/vimentin-positive cells in the total vimentin-positive cell population in the dermis of the mice (12 weeks old) with E-BMT. After evaluation of six different, randomly selected microscopic fields of the skin specimens, ~0.3% of the vimentin-positive cells were also shown to be GFP-positive. Collectively, BMDFs were estimated to represent ~0.5% of the dermal fibroblast population in the skin of E-BMT mice.

E-BMT Improves Survival and Lessens the Severity of Skin Phenotype of DEB Mice by Providing BMDFs to the Skin

Finally, we evaluated the therapeutic potential of E-BMT to ameliorate pathogenic phenotypes of genetic skin diseases with fibroblast dysfunction by providing immunologically tolerated functional BMDFs to the skin. For this purpose, we performed E-BMT on DEB model mice with absent expression of type VII collagen, an adhesion molecule synthesized by both dermal fibroblasts and epidermal keratinocytes. E-BMT to the DEB mouse embryos prevented their neonatal death, which usually occurs within the first 2 days of birth (Figure 6A). Chimerism with GFP$^+$ cells was also confirmed in the BMCs of the DEB mice with E-BMT (Figure 6B). Careful examination of the DEB mice with E-BMT revealed that these mice survived until 17 to 19 days of age, although none of them survived beyond 3 weeks (Figure 6C). RT-PCR analysis showed that type VII collagen expression was clearly detectable in the skin of DEB mice with E-BMT of GFP-transgenic BMCs, but not in the skin of DEB mice without E-BMT (Figure 6D). Immunohistochemical examination showed that type VII collagen, which is normally expressed in the basement membrane region of the dermo-epidermal junction and around the hair follicles of the skin (Figure 6E), but lost in the DEB mouse skin (Figure 6F), was restored in the vicinity of dermal GFP$^+$ cells, possibly BMDFs. This observation was particularly evident in the follicular basement membrane region of the skin of DEB mice with E-BMT (Figure 6, G–P). However, dermo-epidermal separation, characteristic of DEB neonatal mice (Figure 6Q), was lessened but not entirely reversed in the DEB mice with E-BMT (Figure 6R).

Figure 6. E-BMT ameliorates defects in DEB mice after birth. **A:** Relatively long survival of the DEB mice with E-BMT. On the left side is a DEB mouse without E-BMT that died right after the delivery and on the right side is a DEB mouse with E-BMT (**white arrow**) that survived the neonatal period. **B:** BM showed a chimerical condition with GFP$^+$ cells derived from E-BMT. **C:** Comparison of the survival of DEB mice with or without E-BMT. Note that significant improvement in survival after birth was obtained in the mice with E-BMT ($P < 0.01$). **D:** RT-PCR analysis for type VII collagen mRNA expression in the skin of GFP-transgenic mice (**lane a**), DEB mice with E-BMT of GFP-transgenic BMCs (**lane b**), and DEB mice without E-BMT (**lane c**). Immunostaining for type VII collagen in the skin of normal mice (**E**), DEB mice (**F**), and DEB mice with E-BMT of GFP-transgenic BMCs (**G**, **H**). Low magnification (**G**, in the **white circle**), middle magnification (**H**), and high magnification (**I–L**) indicate type VII collagen expression, particularly along the hair follicle structure in association with GFP$^+$ BMDFs. **I:** 4,6-Diamidine-2-phenylindole dihydrochloride staining. **J:** GFP fluorescence. **K:** Type VII collagen staining. **L:** Merger of **I–K**. **M** and **N:** Keratin 5 expression in the follicular keratinocytes beside the BMDFs in the serial skin section compared to that of **I–N**. **M:** Keratin 5 staining. **N:** Merger of **M** and **N**. **O** and **P** indicate type VII collagen expression clearly around the hair follicle structure. H&E staining of the skin sections from DEB mice after birth with no E-BMT (**Q**), and with E-BMT (4 weeks after E-BMT) (**R**). **Asterisks** indicate dermo-epidermal separation. Original magnifications: ×80 (**B**), ×200 (**E**, **H**); ×240 (**F**); ×400 (**E–G**, **I–P**); ×100 (**Q**, **R**).

Discussion

In this study, we have demonstrated, for the first time, that adult BMC transplantation into the fetal circulation via the vitelline vein at embryonic day 13 can provide a significant number of BMDFs into the skin under physiological conditions, and that these BMDFs clearly persist in the skin beyond birth. Transfer of cultured fibroblasts or BM-derived mesenchymal stem cells (in amounts more than 0.5×10^6) to the embryonic circulation via the vitelline vein always resulted in embryonic death (see Supplemental Figure S2 at *http://ajp.amjpathol.org*), possibly attributable to emboli in the microcirculation reflecting the cohesive nature of the cultured mesenchymal cells. These observations imply an apparent advantage of BMCs as compared to cultured fibroblasts or mesenchymal stem cells for embryonic transfer into circulation to generate *de novo* dermal fibroblasts.

BMDFs were not identified either in the transplanted BMC population or in the skin of the E-BMT mouse immediately after birth (data not shown), suggesting that progenitors of the BMDFs exist in the transplanted BM, which then migrate to the uninjured skin, and require appropriate matrix stimulation in the growing skin to become fibroblasts. Fetal mouse skin undergoes rapid growth in conjunction with mesenchymal maturation, processes in which stem cells can differentiate to adipose tissue, smooth muscle cells, and fibroblasts in the dermal matrix.[26,27] Because BM has been shown to contain mesenchymal stem cells,[28–30] transplanted BMCs in the fetal circulation may induce migration of the BM mesenchymal stem cells to the skin with recruiting signals derived from the growing skin.

In this context, it should be noted that E-BMT provided BMDFs to the skin preferentially around hair follicle structures of in both normal and DEB mice. In conjunction with the observation that BMDFs were rarely detected in esophageal lamina propria of normal mice with E-BMT (a few BMDFs were detected in only 1 microscopic field examined of 100 esophageal histological sections; see Supplemental Figure S3 at *http://ajp.amjpathol.org*), we speculate that the developmental stage and/or the growth stage of hair follicles may specifically determine expression of chemoattractants to recruit circulating BMDF progenitor/stem cells to the follicular regions in the skin.

Recently, we reported that bone morphogenic protein-2 (BMP-2) stimulation in muscle tissue recruits BM-derived circulating mesenchymal stem/progenitor cells to form ectopic bone.[31] Because BMP-2 has also been shown to contribute to fetal skin development,[32] this morphogen may also have a role in recruiting circulating mesenchymal stem/progenitor cells to the fetal skin to generate BMDFs after birth. Further investigation is necessary to disclose the precise mechanisms that generate BMDFs in growing, uninjured skin by E-BMT.[33]

Our results presented in this report also suggest the possibility that E-BMT may be a therapeutic option for heritable skin diseases that are caused by genetic dysfunction of skin fibroblasts. To assess this possibility, we performed E-BMT to evaluate the therapeutic efficacy on the mouse model of DEB, characterized by blistering and ulcerations of the skin because of dermo-epidermal separation as a result of homozygous ablation of the type VII collagen gene, Col7a1.[34] This mouse model recapitulates the clinical, genetic, histopathological, and ultrastructural features of human recessively inherited HS-RDEB. Type VII collagen is physiologically located in the basement membrane zone of the skin and the esophagus, and it secures adhesion of the corresponding epithelial tissues to the underlying mesenchyme through formation of anchoring fibrils.[35–37] Because of decreased or absent type VII collagen, patients with DEB suffer from severe burn-like skin lesions, such as blisters, ulcers, and extensive scarring, as a result of minor external trauma throughout their entire life.[38] The severe scar formation of the skin is also associated with a high risk of squamous cell carcinoma in patients with RDEB.[39,40] In some cases, swallowing of solid food may induce separation of the epithelial mucosa of the esophagus and repeated formation of esophageal ulcers may eventually lead to scar-induced constrictions, resulting in difficulty in eating. Mice with DEB will also have a feeding difficulties from the birth on, because of oral blisters and ulcers, resulting in premature demise within a few days of birth.[34] Type VII collagen is known to be produced by both epidermal keratinocytes and dermal fibroblasts,[17–19] and supplementation of normal fibroblasts to the lesional skin from patients with DEB transplanted on nude mice has been shown to rescue skin phenotypes by providing type VII collagen.[20]

Here, we demonstrated that E-BMT to the DEB mouse embryos provides BMDFs expressing type VII collagen in the skin and ameliorates the phenotypic severity, at least in part, by providing type VII collagen to the skin. As demonstrated above, BMDFs were predominately in the areas adjacent to hair follicles and barely detectable in the interfollicular region of the dermo-epidermal junction (see Supplemental Figure S1 at *http://ajp.amjpathol.org*). Because their preferential migration to the areas surrounding hair follicles, localized dermo-epidermal separation was still evident in the DEB mice with E-BMT at 3 weeks after birth (Figure 6R). We could not observe fully developed, mature anchoring fibrils that are formed from type VII collagen at the basement membrane region, by transmission electron microscopy (see Supplemental Figure S4A at *http://ajp.amjpathol.org*). However, we observed fibrillar structures, which may represent immature anchoring fibrils, at localized portions of the cutaneous basement membrane zone of the skin of the DEB mice with E-BMT (see Supplemental Figure S4B at *http://ajp.amjpathol.org*). Based on these observations, coupled with significant improvement in the survival of the newborn DEB mice with E-BMT, we believe that BMDFs, while providing type VII collagen molecules to the cutaneous basement membrane zone, contributed to some extent to improvement of the disease phenotype in DEB mice.

All DEB mice with E-BMT died at ~3 weeks after birth, at the time they start feeding on solid food. The limited number of the transplanted BMCs in the embryo might not be sufficient to provide an adequate number of type VII collagen-producing fibroblasts to the esophagus to

allow eating solid food. Indeed, the relative number of BMDFs in the mouse esophagus elicited by E-BMT was less than one-hundredth of the number of BMDFs in the skin (see Supplemental Figure S3 at *http://ajp.amjpathol.org*). Nevertheless, we believe that our data provide a future perspective for application of E-BMT to the patients with DEB *in utero* when prenatal diagnosis indicates COL7A1 mutations, with predicted severe phenotype.

BMT is a well-established medical intervention for both children and adults afflicted with severe hematopoietic diseases, such as leukemia. However, there are still difficulties in finding HLA-matched donors for BMT. Therefore, patients must undergo treatment by irradiation and/or myeloablative reagents, in combination with immune suppressive therapies to prevent immune rejection reaction and to avoid graft-versus-host disease, before BMT can be performed. On the other hand, during the first trimester of human gestation the fetus has been shown to accept allogenic antigens by introducing immunological tolerance with clonal deletion of the allogenic antigen-reacting lymphocytes in the thymus.[41] During this time period, E-BMT without matching HLA to the recipient is expected to successfully engraft without the need of myeloablative or immunosuppressive regimen.[42] E-BMT in this time period can also be expected to introduce immune tolerance to a molecule that is expressed in the donor cells but not in the fetus because of genetic mutations.

Our results suggest that E-BMT can be an effective therapeutic option not only by providing functional fibroblasts to the lesional tissues, such as the skin, but also by introducing immune tolerance against the exogenously provided molecules (GFP) expressed in the donor cells, thus resulting in long-term survival of the GFP-expressing BMDFs in the recipient skin. On the other hand, subcutaneous transfer of various GFP^+ cells, including BMCs and mesenchymal stem cells, failed to generate immune tolerance against GFP, demonstrating an advantage of E-BMT at least for tolerance induction against exogenous immunogenic molecules.

Our study also suggests that a limited number of BMCs may be sufficient to introduce immune tolerance against the molecules initially absent in the recipients if E-BMT is performed at the appropriate time frame in gestation with HLA-matched donor cells. A recent animal study suggested that allogenic BMCs may have short survival after birth as compared to congenic BMCs, even by E-BMT.[12] Other experimental and clinical studies have shown, however, that successful renal transplantation from HLA-mismatched donors can be achieved when combined with transplantation of hematopoietic stem cells from the same donors by nonmyeloablative conditioning, resulting in discontinuation of all immunosuppressive therapies afterward.[43] The report of these clinical trials suggested that initial transient BM chimerism of the recipient hematopoietic tissues with transplanted donor hematopoietic stem cells may be sufficient to induce central and/or peripheral immune tolerance to ensure stable maintenance of the transplanted allogenic kidney. In this context, E-BMT may introduce immune tolerance against type VII collagen in DEB patients who initially lack this protein because of genetic mutations in the COL7A1 gene. If this is indeed the case, E-BMT may be established as an essential therapeutic option for severe HS-RDEB patients *in utero* to allow them to receive extensive gene-, cell-, or protein-based molecular therapies to cure the disease after birth.[23]

Concerning the technical aspect of E-BMT, some human inherited diseases, such as hematological disorders (eg, Fanconi's anemia and thalassemia), immunological defects (eg, SCID), or metabolic diseases (eg, Hurler and Krabbe diseases) have already been clinically treated by E-BMT.[13] In these diseases, E-BMT was shown to preserve the organ function. If BMC transplantation is performed postnatally, radiation therapy, intensive immunosuppression, and myeloablation have to be used to minimize the risk of rejection or graft-versus-host disease. For these reasons, we believe that E-BMT may have a rational advantage for treatment of EB patients as compared to postnatal BMT with immunosuppressive regimen. Such postnatal immunosuppressive procedures potentially have a high risk to induce severe cutaneous, and possibly systemic, infection in EB patients with multiple skin ulcers over the entire body surface.

E-BMT with self-BMCs transduced with a therapeutic gene would seem to be an ideal option for future embryonic gene therapy toward genetic skin diseases, provided that self-BMCs can be obtained from the fetus. Further continuous efforts of basic and clinical studies are required to establish E-BMT as an essential therapeutic strategy for currently intractable genetic diseases, such as DEB.

References

1. Iwano M, Plieth D, Danoff TM, Xue C, Okada H, Neilson EG: Evidence that fibroblasts derive from epithelium during tissue fibrosis. J Clin Invest 2002, 110:341–350
2. Ishii G, Sangai T, Oda T, Aoyagi Y, Hasebe T, Kanomata N, Endoh Y, Okumura C, Okuhara Y, Magae J, Emura M, Ochiya T, Ochiai A: Bone-marrow-derived myofibroblasts contribute to the cancer-induced stromal reaction. Biochem Biophys Res Commun 2003, 309:232–240
3. Brittan M, Hunt T, Jeffery R, Poulsom R, Forbes SJ, Hodivala-Dilke K, Goldman J, Alison MR, Wright NA: Bone marrow derivation of pericryptal myofibroblasts in the mouse and human small intestine and colon. Gut 2002, 50:752–757
4. Direkze NC, Forbes SJ, Brittan M, Hunt T, Jeffery R, Preston SL, Poulsom R, Hodivala-Dilke K, Alison MR, Wright NA: Multiple organ engraftment by bone-marrow-derived myofibroblasts and fibroblasts in bone-marrow-transplanted mice. Stem Cells 2003, 21:514–520
5. Hashimoto N, Jin H, Liu T, Chensue SW, Phan SH: Bone marrow-derived progenitor cells in pulmonary fibrosis. J Clin Invest 2004, 113:243–252
6. Ogawa M, LaRue AC, Drake CJ: Hematopoietic origin of fibroblasts/myofibroblasts: its pathophysiologic implications. Blood 2006, 108:2893–2896
7. LaRue AC, Masuya M, Ebihara Y, Fleming PA, Visconti RP, Minamiguchi H, Ogawa M, Drake CJ: Hematopoietic origins of fibroblasts: I. In vivo studies of fibroblasts associated with solid tumors. Exp Hematol 2006, 34:208–218
8. Opalenik SR, Davidson JM: Fibroblast differentiation of bone marrow-derived cells during wound repair. FASEB J 2005, 19:1561–1563
9. Ishii G, Sangai T, Sugiyama K, Ito T, Hasebe T, Endoh Y, Magae J, Ochiai A: In vivo characterization of bone marrow-derived fibroblasts recruited into fibrotic lesions. Stem Cells 2005, 23:699–706

10. Flake AW: In utero transplantation of haemopoietic stem cells. Best Pract Res Clin Haematol 2001, 14:671–683
11. Javazon EH, Merchant AM, Danzer E, Flake AW: Reconstitution of hematopoiesis following intrauterine transplantation of stem cells. Methods Mol Med 2005, 105:81–94
12. Peranteau WH, Endo M, Adibe OO, Flake AW: Evidence for an immune barrier after in utero hematopoietic-cell transplantation. Blood 2007, 109:1331–1333
13. Troeger C, Surbek D, Schoberlein A, Schatt S, Dudler L, Hahn S, Holzgreve W: In utero haematopoietic stem cell transplantation. Experiences in mice, sheep and humans. Swiss Med Wkly 2006, 136:498–503
14. Briggaman RA, Wheeler Jr CE: The epidermal-dermal junction. J Invest Dermatol 1975, 65:71–84
15. Lunstrum GP, Kuo HJ, Rosenbaum LM, Keene DR, Glanville RW, Sakai LY, Burgeson RE: Anchoring fibrils contain the carboxyl-terminal globular domain of type VII procollagen, but lack the amino-terminal globular domain. J Biol Chem 1987, 262:13706–13712
16. Sakai LY, Keene DR, Morris NP, Burgeson RE: Type VII collagen is a major structural component of anchoring fibrils. J Cell Biol 1986, 103:1577–1586
17. Stanley JR, Rubinstein N, Klaus-Kovtun V: Epidermolysis bullosa acquisita antigen is synthesized by both human keratinocytes and human dermal fibroblasts. J Invest Dermatol 1985, 85:542–545
18. Ryynanen J, Sollberg S, Parente MG, Chung LC, Christiano AM, Uitto J: Type VII collagen gene expression by cultured human cells and in fetal skin. Abundant mRNA and protein levels in epidermal keratinocytes. J Clin Invest 1992, 89:163–168
19. Woodley DT, Briggaman RA, Gammon WR, O'Keefe EJ: Epidermolysis bullosa acquisita antigen is synthesized by human keratinocytes cultured in serum-free medium. Biochem Biophys Res Commun 1985, 130:1267–1272
20. Woodley DT, Krueger GG, Jorgensen CM, Fairley JA, Atha T, Huang Y, Chan L, Keene DR, Chen M: Normal and gene-corrected dystrophic epidermolysis bullosa fibroblasts alone can produce type VII collagen at the basement membrane zone. J Invest Dermatol 2003, 121:1021–1028
21. Woodley DT, Remington J, Huang Y, Hou Y, Li W, Keene DR, Chen M: Intravenously injected human fibroblasts home to skin wounds, deliver type VII collagen, and promote wound healing. Mol Ther 2007, 15:628–635
22. Goto M, Sawamura D, Ito K, Abe M, Nishie W, Sakai K, Shibaki A, Akiyama M, Shimizu H: Fibroblasts show more potential as target cells than keratinocytes in COL7A1 gene therapy of dystrophic epidermolysis bullosa. J Invest Dermatol 2006, 126:766–772
23. Wong T, Gammon L, Liu L, Mellerio JE, Dopping-Hepenstal PJ, Pacy J, Elia G, Jeffery R, Leigh IM, Navsaria H, McGrath JA: Potential of fibroblast cell therapy for recessive dystrophic epidermolysis bullosa. J Invest Dermatol 2008 Apr. 3 [Epub ahead of print]
24. Chen M, Woodley DT: Fibroblasts as target cells for DEB gene therapy. J Invest Dermatol 2006, 126:708–710
25. Stripecke R, Carmen Villacres M, Skelton D, Satake N, Halene S, Kohn D: Immune response to green fluorescent protein: implications for gene therapy. Gene Ther 1999, 6:1305–1312
26. Van Exan RJ, Hardy MH: The differentiation of the dermis in the laboratory mouse. Am J Anat 1984, 169:149–164
27. Breathnach AS: Development and differentiation of dermal cells in man. J Invest Dermatol 1978, 71:2–8
28. Prockop DJ: Marrow stromal cells as stem cells for nonhematopoietic tissues. Science 1997, 276:71–74
29. Pittenger MF, Mackay AM, Beck SC, Jaiswal RK, Douglas R, Mosca JD, Moorman MA, Simonetti DW, Craig S, Marshak DR: Multilineage potential of adult human mesenchymal stem cells. Science 1999, 284:143–147
30. Jiang Y, Jahagirdar BN, Reinhardt RL, Schwartz RE, Keene CD, Ortiz-Gonzalez XR, Reyes M, Lenvik T, Lund T, Blackstad M, Du J, Aldrich S, Lisberg A, Low WC, Largaespada DA, Verfaillie CM: Pluripotency of mesenchymal stem cells derived from adult marrow. Nature 2002, 418:41–49
31. Otsuru S, Tamai K, Yamazaki T, Yoshikawa H, Kaneda Y: Bone marrow-derived osteoblast progenitor cells in circulating blood contribute to ectopic bone formation in mice. Biochem Biophys Res Commun 2007, 354:453–458
32. Stelnicki EJ, Longaker MT, Holmes D, Vanderwall K, Harrison MR, Largman C, Hoffman WY: Bone morphogenetic protein-2 induces scar formation and skin maturation in the second trimester fetus. Plast Reconstr Surg 1998, 101:12–19
33. Ebihara Y, Masuya M, Larue AC, Fleming PA, Visconti RP, Minamiguchi H, Drake CJ, Ogawa M: Hematopoietic origins of fibroblasts: II. In vitro studies of fibroblasts, CFU-F, and fibrocytes. Exp Hematol 2006, 34:219–229
34. Heinonen S, Mannikko M, Klement JF, Whitaker-Menezes D, Murphy GF, Uitto J: Targeted inactivation of the type VII collagen gene (Col7a1) in mice results in severe blistering phenotype: a model for recessive dystrophic epidermolysis bullosa. J Cell Sci 1999, 112:3641–3648
35. Bächinger HP, Morris NP, Lunstrum GP, Keene DR, Rosenbaum LM, Compton LA, Burgeson RE: The relationship of the biophysical and biochemical characteristics of type VII collagen to the function of anchoring fibrils. J Biol Chem 1990, 265:10095–10101
36. Uitto J, Chung-Honet LC, Christiano AM: Molecular biology and pathology of type VII collagen. Exp Dermatol 1992, 1:2–11
37. Burgeson RE: Type VII collagen, anchoring fibrils, and epidermolysis bullosa. J Invest Dermatol 1993, 101:252–255
38. Horn HM, Tidman MJ: The clinical spectrum of dystrophic epidermolysis bullosa. Br J Dermatol 2002, 146:267–274
39. Yamada M, Hatta N, Sogo K, Komura K, Hamaguchi Y, Takehara K: Management of squamous cell carcinoma in a patient with recessive-type epidermolysis bullosa dystrophica. Dermatol Surg 2004, 30:1424–1429
40. Pourreyron C, Cox G, Mao X, Volz A, Baksh N, Wong T, Fassihi H, Arita K, O'Toole EA, Ocampo-Candiani J, Chen M, Hart IR, Bruckner-Tuderman L, Salas-Alanis JC, McGrath JA, Leigh IM, South AP: Patients with recessive dystrophic epidermolysis bullosa develop squamous-cell carcinoma regardless of type VII collagen expression. J Invest Dermatol 2007, 127:2438–2444
41. Billingham RE, Brent L, Medawar PB: 'Actively acquired tolerance' of foreign cells 1. Transplantation 2003, 76:1409–1412
42. Flake AW, Zanjani ED: In utero hematopoietic stem cell transplantation: ontogenic opportunities and biologic barriers. Blood 1999, 94:2179–2191
43. Kawai T, Cosimi AB, Spitzer TR, Tolkoff-Rubin N, Suthanthiran M, Saidman SL, Shaffer J, Preffer FI, Ding R, Sharma V, Fishman JA, Dey B, Ko DS, Hertl M, Goes NB, Wong W, Williams Jr WW, Colvin RB, Sykes M, Sachs DH: HLA-mismatched renal transplantation without maintenance immunosuppression. N Engl J Med 2008, 358:353–361

doi: 10.1111/j.1346-8138.2008.00479.x

CASE REPORT

Significance of sentinel node biopsy in the management of squamous cell carcinoma arising from recessive dystrophic epidermolysis bullosa

Akiko ROKUNOHE,[1] Hajime NAKANO,[1] Takayuki AIZU,[1] Takahide KANEKO,[1] Koji NAKAJIMA,[1] Satsuki IKENAGA,[1] Yasushi MATSUZAKI,[1] Takaya MURAI,[1] Katsuto TAMAI,[2] Daisuke SAWAMURA[1]

[1]*Department of Dermatology, Hirosaki University Graduate School of Medicine, Hirosaki, and* [2]*Division of Gene Therapy Science, Osaka University Graduate School of Medicine, Osaka, Japan*

ABSTRACT

The most life-threatening complication developing in patients with recessive dystrophic epidermolysis bullosa (RDEB) is squamous cell carcinoma (SCC). To improve patient prognosis, early detection of regional lymph node metastasis is required. Herein, we report a patient diagnosed with non-Hallopeau–Siemens RDEB who developed SCC on the left foot with inguinal lymph node swelling. Use of the sentinel node biopsy (SNB) technique favorably minimized defective damage to the inguinal region in this case. Genetic analysis identified one novel *COL7A1* mutation, a maternal c.238G > C (p.A80P) and one previously reported mutation, a paternal c.3631C > T (p.Q1211X). A published work review demonstrated that no *COL7A1* mutations specific for SCC development in RDEB have previously been identified. It remains unclear if SNB in combination with gene diagnosis is beneficial for the management of SCC in RDEB patients, however, because of the limited number of case reports. To address this issue, *COL7A1* mutational analysis should be performed in as many cases of RDEB as possible.

Key words: *COL7A1*, dystrophic epidermolysis bullosa, mutation, sentinel node biopsy, squamous cell carcinoma.

INTRODUCTION

Dystrophic epidermolysis bullosa (DEB) is a rare inherited skin disease characterized by the formation of blisters below the lamina densa of the basement membrane. This separation results from mutations in the type VII collagen gene (*COL7A1*) resulting in a lack of or aberrant anchoring fibrils (AF). DEB can be inherited as either an autosomal dominant or autosomal recessive disorder. Recessive DEB (RDEB) is classified into two subtypes, Hallopeau-Siemens (RDEB-HS) and non-Hallopeau–Siemens (RDEB-nHS); the former lacks AF, while the latter exhibits reduced or rudimentary-appearing AF.[1] Although RDEB-HS typically displays a more severe phenotype, both forms of RDEB can present with chronic mucocutaneous erosions or ulcers, atrophic scarring, multiple milia, pseudosyndactyly, nail dystrophy, scarring alopecia, esophageal stenosis and dental deformities. Recurrent denudation of the skin with chronic inflammation in severe RDEB causes hypochromic anemia and growth retardation and requires life-long medical care. The most life-threatening complication of RDEB, however, is squamous cell carcinoma (SCC). Recently, several case reports have suggested a role for sentinel node biopsy (SNB) in the early detection of micrometastases of SCC arising in the setting of RDEB.[2–4] Herein, we report a patient with RDEB-nHS, a compound heterozygote harboring two *COL7A1* mutations, complicated by recurrent SCC, in which SNB was performed. We discuss the roles of SNB in combination with COL7A1

Correspondence: Hajime Nakano, M.D., Department of Dermatology, Hirosaki University Graduate School of Medicine, 5 Zaifu-cho, Hirosaki 036-8562, Japan. Email: hnakano@cc.hirosaki-u.ac.jp

Received 1 October 2007; accepted 29 February 2008.

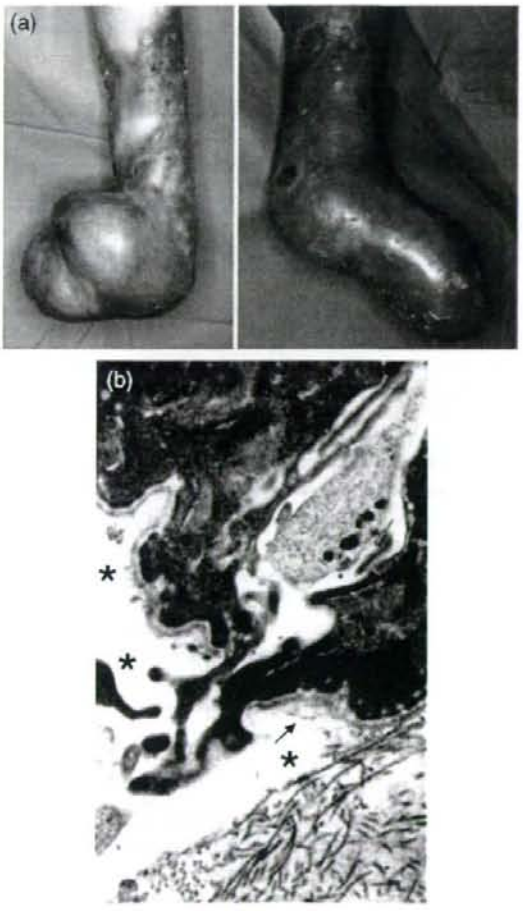

Figure 1. (a) Clinical findings of our patient with recessive dystrophic epidermolysis bullosa. The patient's right hand (left panel) and foot (right panel) exhibit pseudosyndactyly. (b) Transmission electron microscopy of uninvolved forearm skin demonstrates blister formation beneath the lamina densa (asterisk). The arrow indicates rudimentary anchoring fibrils.

mutational analysis in the management of cutaneous tumors arising in the blistering genodermatoses.

CASE REPORT

A 27-year-old Japanese man, who had been diagnosed with RDEB soon after birth, initially presented to us with a 4-month history of intractable ulcer on his left foot. He provided a history of recurring generalized mucocutaneous blistering and erosions

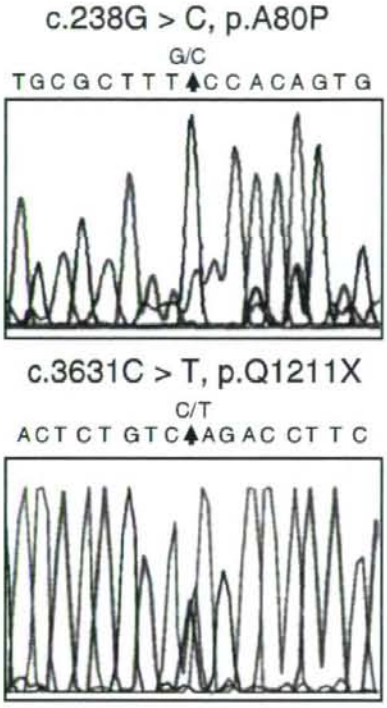

Figure 2. Direct sequencing identified a maternal missense mutation c.238G > C (upper) and a paternal nonsense mutation c.3631C > T (lower).

since birth. His hands and feet exhibited pseudosyndactyly and complete nail loss (Fig. 1a). There were variably sized erosions with atrophic scarring and multiple milia over the trunk and extremities. Severe scarring was observed throughout, but most prominently over the lower extremities. Hematological examination revealed hypochromic anemia, thrombocytosis and leukocytosis. Esophageal stenosis was demonstrated by X-ray analysis. At 20 years of age, he was diagnosed with a well-differentiated SCC on the left prepatellar region. He underwent tumor resection and full-thickness skin graft at that time. Electron microscopy confirmed cleavage below the lamina densa and reduced, rudimentary AF (Fig. 1b). Genetic analysis[5] identified one novel *COL7A1* mutation, a maternal c.238G > C (p.A80P) and one previously reported mutation, a paternal c.3631C > T (p.Q1211X[6]) (Fig. 2). Those mutations were not detected in any of 102 healthy controls.

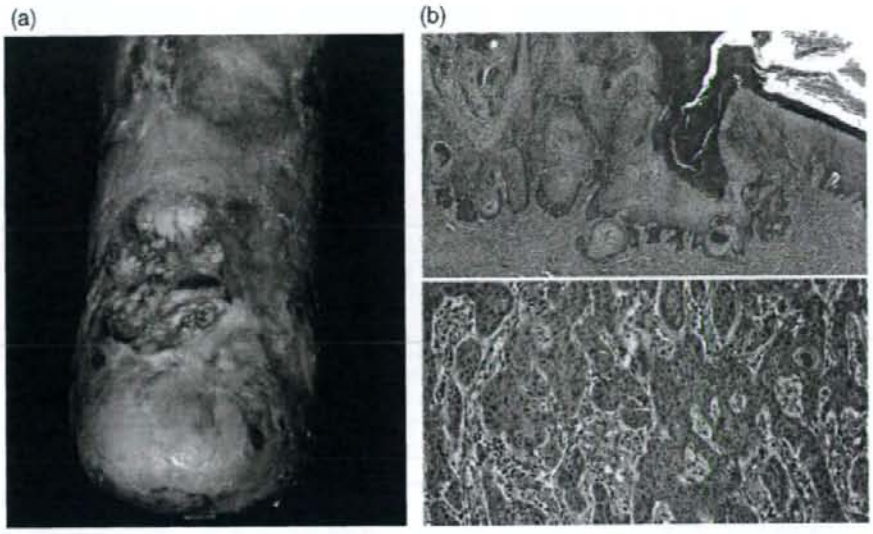

Figure 3. (a) A hyperkeratotic and encrusted granulomatous growth of the left instep. (b) Light microscopy demonstrated a well-differentiated squamous cell carcinoma with hyperkeratosis and horn pearls (upper panel; HE stain, original magnification ×20). Invading, proliferating atypical keratinocytes were observed at the base of the tumor mass (lower panel; HE stain, original magnification ×100).

On presentation, we observed a non-healing erosive area measuring 6 cm × 4 cm with hyperkeratotic crusting and hypertrophic granulation on the left instep (Fig. 3a). Three firm subcutaneous nodules were palpable in the left femoroinguinal region. Histological analysis of the granulomatous lesion demonstrated a well-differentiated SCC (Fig. 3b). Based on the clinical course and laboratory findings, we made a diagnosis of RDEB-nHS associated with well-differentiated SCC. After excision of the tumor with a 1.5-cm margin, the defect was repaired with a full-thickness skin graft. To distinguish lymphadenopathy due to an inflammatory process from possible SCC lymph node metastases, we performed a sentinel node biopsy according to a minor modification of the standard procedure.[7] Briefly, 3 h prior to surgery, the patient underwent lymphoscintigraphy using an i.d. injection of ^{99m}Tc-phytate at four points around the tumor. Dynamic and static imaging was performed for 2 h with a γ camera to identify focal accumulations of radioactive tracer in the regional lymph node basin. Three sentinel nodes, corresponding with the three subcutaneous nodules detected on palpation, were identified and removed. Histopathology revealed nonspecific inflammation with no evidence of metastasis of SCC.

DISCUSSION

Patients with RDEB are at increased risk of developing SCC, a life-threatening disease. The cumulative risks for death from SCC in RDEB-HS and all other RDEB subtypes by age 45 are 55.2% and 12.8%, respectively.[8] Although the SCC that arise in RDEB are typically well-differentiated, these lesions can exhibit rapid proliferation and frequent metastasis.[9] The presence of regional lymph node metastasis is the most important prognostic factor for the majority of solid tumors, including SCC. Therefore, early detection of regional lymph node metastasis will help to improve patient prognosis.

Recent studies have demonstrated that SNB can detect subclinical lymph node metastasis in patients with high-risk cutaneous SCC.[7] RDEB patients should be classified to this group because of the aggressiveness of associated SCC.[9] Previously, SNB has been applied to patients with occult regional lymph node metastasis; those patients displaying

Table 1. Clinical features and *COL7A1* genotype of recessive dystrophic epidermolysis bullosa patients bearing squamous cell carcinoma in which at least one mutation was identified

Patient	Age	Gender	Subtype	Mutation	Consequences	NC1	Reference
1	12	M	nHS	p.G2575R/p.E2857X	mis/PTC	+	Kawasaki *et al.*[14]
2	36	M	HS	c.4249delA/nd	PTC/nd	+	Ortiz-Urda *et al.*[11]
3	39	F	HS	p.A425G/p.A425G	mis/mis	+	Ortiz-Urda *et al.*[11]
4	35	F	HS	p.R525X/p.R578X	PTC/PTC	−	Pourreyron *et al.*[12]
5	29	F	HS	p.R525X/p.Q905X	PTC/PTC	−	Pourreyron *et al.*[12]
6	54	M	HS	c.3832-1G > A/nd	PTC/nd	+	Pourreyron *et al.*[12]
7	42	F	nHS	c.6075delC/nd	PTC/nd	+	Pourreyron *et al.*[12]
8	33	F	nHS	c.3839delC/c.6501G > A	PTC/IFD	+	Pourreyron *et al.*[12]
9	32	M	HS	c.8244insC/c.8244insC	PTC/PTC	+	Pourreyron *et al.*[12]
10	43	M	HS	p.R578X/c.7786delG	PTC/PTC	+	Pourreyron *et al.*[12]
11	26	M	HS	c.6501 + 1G > C/nd	IFD/nd	+	Pourreyron *et al.*[12]
12	26	M	nHS	c.5572delG/p.G1703E	IFD/nd	+	Pourreyron *et al.*[12]
13	38	F	HS	p.G2073D/p.R578X	mis/PTC	+	Pourreyron *et al.*[12]
14	20	M	nHS	p.A80P/p.Q1211X	mis/PTC	+	Present case

IFD, in-frame deletion; mis, missense; nd, not determined; PTC, premature termination codon.

clinically overt lymphadenopathy have typically undergone complete lymph node dissection. Such an extensive procedure, however, may not always be indicated for RDEB patients with SCC, as the regional lymph nodes in these patients are frequently enlarged due to associated persistent inflammation or chronic infection. This clinical situation makes it difficult to distinguish nonspecific inflammatory lymphadenopathy from lymph node metastasis. In previous case reports, SNB has been applied to only three RDEB cases complicated by SCC, one RDEB-nHS[2] and two RDEB-HS.[3,4] It should be noted that precise injection of tracer into the intradermal space in patients with RDEB is more difficult than injection into normal skin due to the severe scarring and atrophy of peritumoral skin. In this case, three sentinel nodes were resected with limited incision of the overlying skin. All three nodes were found to be tumor-negative, therefore subsequent therapeutic lymph node dissection was not required. Overall, the SNB technique minimized the damage to the inguinal region in this patient.

While greater than 50% RDEB-HS patients die from SCC by age 45, a subset of patients with this disease do not develop SCC, suggesting that some RDEB patients may be more susceptible to SCC development.[10] The molecular mechanism that predisposes patients to skin neoplasms was not well understood until Ortiz-Urda *et al.* revealed that a fragment of type VII collagen spanning from amino acids 760–1050 is critical in tumorigenesis.[11] This fragment, which contains the fibronectin III-like repeats (FNC1) of the non-collagenous domain NC1, is required for the Ras-driven tumorigenesis in cultured epidermal keratinocytes isolated from RDEB patients.[11] The two *COL7A1* mutations in our patient, a maternal c.238G > C (p.A80P) and a paternal c.3631C > T (p.Q1211X), are predicted to express an amino acid-substituted and truncated collagen VII proteins, respectively, both of which contain intact FNC1. These findings suggest that increased susceptibility to SCC in our patient may be explained by the activation of the Ras mitogenic pathway, as predicted by the theory of tumorigenesis in RDEB proposed by Ortiz-Urda *et al.*[11] A recent study by Pourreyron *et al.*, however, demonstrated that two of 11 RDEB patients developing SCC did not express detectable levels of collagen VII protein in the tumors by immunohistochemistry and Western blotting (Table 1, patients 4 and 5).[12] These data imply that additional genetic or epigenetic factors are involved in the increased incidence of SCC in this blistering disease. It will be interesting to determine the relationship between *COL7A1* genotype and the characteristics of SCC lesions arising in RDEB, such as recurrence, invasiveness and metastasis. *COL7A1* mutations have been identified in at least one allele in 14 cases of RDEB with SCC examined (Table 1). No particular mutation, however, has been found to be specific for the development of SCC with RDEB.